Title Page

The roles of cell signaling pathways in cell-to-cell contact-mediated Epstein–Barr virus transmission

Asuka Nanbo[1]*, Haruna Terada[1]†, Kunihiro Kachi[1], Kenzo Takada[2], and Tadashi Matsuda[1]

Graduate School of Pharmaceutical Sciences, Hokkaido University, N12 W6, Kita-ku, 060-0812 Sapporo, Japan[1], and Institute for Genetic Medicine, Hokkaido University, N15 W7, Kita-ku, 060-8638 Sapporo, Japan[2]

Running title; Mechanism of cell-to-cell contact-mediated EBV transmission

*Corresponding author.

Mailing address: Graduate School of Pharmaceutical Sciences, Hokkaido University, N12 W6, Kita-ku, 060-0812 Sapporo, Japan.

Phone: +81(11)706-3244

Fax: +81(11)706-4990

Email: nanboa@pharm.hokudai.ac.jp

A.N. and H.T. contributed equally to this manuscript.

†Present address: RIKEN Wako Institute, 2-1 Hirosawa, Wako, Saitama 351-0198, Japan

The word count for the abstract: 250

The word count for the text: 4676

Abstract

Epstein–Barr virus (EBV), a human gamma herpesvirus, establishes a life-long latent infection in B lymphocytes and epithelial cells following primary infection. Several lines of evidence indicate that the efficiency of EBV infection in epithelial cells is accelerated up to 10^4-fold by co-culturing with EBV-infected Burkitt's lymphoma (BL) cells compared with infection with cell-free virions, indicating that EBV infection into epithelial cells is mainly mediated *via* cell-to-cell contact. However the molecular mechanisms involved in this pathway are poorly understood. Here we establish a novel assay to assess cell-to-cell contact-mediated EBV transmission by co-culturing an EBV-infected BL cell line with an EBV-negative epithelial cell line under the stimulation for lytic cycle induction. By using the assay we confirmed that EBV was transmitted from BL cells to epithelial cells *via* cell-to-cell contact but not *via* cell-to-cell fusion. The inhibitor treatments of extracellular signal-regulated kinase (ERK) and nuclear factor (NF)-κB pathways blocked EBV transmission in addition to lytic induction. The blockage of phosphoinositide 3-kinase (PI3K) pathway impaired EBV transmission coupled with inhibition of the lytic induction. Knockdown of the RelA/p65 subunit of NF-κB reduced viral transmission. Moreover these signaling pathways were activated in co-cultured BL cells and in epithelial cells. Finally we observed that the viral replication was induced in co-cultured BL

cells. Taken together, our data suggest that cell-to-cell contact induces multiple cell signaling pathways in BL cells and epithelial cells, contributing to the induction of the viral lytic cycle in BL cells and the enhancement of viral transmission to epithelial cells.

Introduction

Epstein–Barr virus (EBV), a human gamma herpesviruses, establishes a persistent latent infection in B lymphocytes and epithelial cells following primary infection (19). EBV has been implicated as a cause of lymphomas and epithelial malignancies such as Burkitt's lymphoma (BL), Hodgkin's disease, nasopharyngeal carcinoma and gastric cancer (19). EBV binds to B lymphocytes through a direct interaction of the EBV glycoprotein gp350/220 with the complement receptor CD21 (13, 22). In contrast, the mechanism by which EBV enters epithelial cells remains undefined. Epithelial cells express very low levels of CD21 or are CD21-negative in culture (12, 15), resulting in the lack of an efficient infection of cell-free viruses.

Several lines of evidence indicate that EBV infection into epithelial cells is mainly mediated by cell-to-cell contact (5, 15, 34, 35, 37, 43). The rate of EBV infection in epithelial cells increases up to 10^3-fold by co-culturing with EBV-positive B cells compared with infection with cell-free EBV (5, 15, 43). Moreover Shannon-Lowe *et al.* demonstrated that most EBV virions are retained on cell surfaces after binding to primary B cells and transferred to epithelial cells, resulting in the 10^3 to 10^4-fold increase of infection compared with cell-free virus infection (35). All these studies support a model that EBV-infected B cells migrating into the epithelial stroma

or intraepithelial space contribute to the efficient EBV transmission into epithelium *via* cell-to-cell contact (42, 43). However the molecular mechanisms of cell-to-cell EBV transmission remain unclear.

In our present study we establish a novel assay to assess cell-to-cell contact-mediated EBV transmission by co-culturing an EBV-infected BL cell line with an EBV-negative epithelial cell line under the stimulation for lytic cycle induction in BL cells. By using the system, we showed that EBV transmission was mediated *via* cell-to-cell contact but not *via* cell-to-cell fusion. We demonstrated that the treatment of inhibitors of extracellular signal-regulated kinase (ERK) and nuclear factor (NF)-κB pathways blocked EBV transmission in addition to lytic induction. The blockage of phosphoinositide 3-kinase (PI3K) pathway impaired EBV transmission coupled with inhibition of the lytic induction. Knockdown of RelA/p65 subunit of NF-κB also reduced the efficiency of viral transmission. Moreover these cell signaling molecules were activated in co-cultured BL cells and epithelial cells. Finally we observed that the viral lytic cycle was induced in BL cells by co-culturing with epithelial cells. The possible roles of these signaling molecules in cell-to-cell contact-mediated EBV transmission are discussed.

Materials and Methods

Cell culture

African green monkey kidney epithelial Vero-E6 cell line (9, 26), which was provided by Dr Ayato Takada, and human gastric adenocarcinoma cell lines, AGS (2, 49) and NU-GC-3 (1, 16, 22, 31, 32, 49) were grown in high-glucose Dulbecco's modified Eagle's medium (DMEM) containing 10% fetal bovine serum (FBS) and antibiotics. BL-derived Akata$^-$EBV-eGFP cells, which are latently infected with a recombinant Akata strain EBV encoding enhanced green fluorescent protein (eGFP) gene inserted into viral BXLF1 ORF (22), were maintained in RPMI-1640 medium containing 10% FBS, antibiotics and 800 μg/ml G418. EBV-positive BL-derived Akata (Akata$^+$) cells (39-41) and EBV-negative BL-derived Daudi (Daudi$^-$) cells (20, 28) were maintained in RPMI-1640 medium containing 10% FBS and antibiotics. Cells were maintained at 37°C in 5% CO_2.

EBV-transmission assay

EBV-negative Vero-E6 cells (5 x 10^4) were co-cultured with Akata$^-$EBV-eGFP cells (5 x 10^5) for 24 h in 24-well plates in the presence or absence of 0.2% F(ab')$_2$ fragments of goat

anti-human IgG polyclonal antibody (αhIgG, DAKO, Glostrup, Denmark) to induce the viral lytic cycle in Akata$^-$EBV-eGFP cells. To remove Akata$^-$EBV-eGFP, Vero-E6 cells were washed, trypsinized, and cultured in 6-well plates for 6 h in the absence of αhIgG. For the transmission assay with a physical barrier, Vero-E6 cells (1 x 10^5) were grown on the basolateral chamber of 24-well plate with membrane inserts with pore sizes of 0.4 μm (Corning, Toledo, USA). Akata$^-$EBV-eGFP cells (1 x 10^5) were added to the membrane inserts and incubated for 24 h in the presence or absence of αhIgG. Vero-E6 cells were grown on the cover slips and fixed in 4% paraformaldehyde (PFA). The transmission of EBV-eGFP into Vero-E6 cells was analyzed by a confocal laser scanning microscope (Fluoview FV10i, Olympus, Tokyo, Japan). Four fields containing approximately 2,000 cells were randomly collected and the fractions of eGFP-positive Vero-E6 cells were measured. The percentages of eGFP-positive cells were also analyzed by flow cytometry (FACSCalibur, Becton, Dickinson and company, Franklin Lakes, New Jersey, USA). In parallel with FACS analysis, the same sample was analyzed by a confocal laser scanning microscope to confirm that the sample did not contain Akata$^-$EBV-eGFP cells.

Immunofluorescent staining

Vero-E6 cells were grown on the cover slips and co-cultured with Akata$^-$EBV-eGFP cells

under the treatment of αhIgG. For analysis of the expression of caveolin-1, EBNA1, and HLA-DR, Vero-E6 cells were washed to remove Akata-EBV-eGFP, cultured in 6-well plates for 6 h and grown on cover slips. For analysis of the phosphorylation of ERK, PI3K and the nuclear translocation of RelA/p65, Vero-E6 cells grown in 35 mm glass-bottomed culture dishes (MatTek corporation, Ashland, USA) were co-cultured with Akata-EBV-eGFP cells in the presence or absence of 0.2% αhIgG for various times. The cells were fixed with 4% PFA in PBS for 10 min at room temperature, permeabilized with PBS containing 0.05% Triton X-100 for 10 min at room temperature and blocked in PBS containing 1% BSA and 0.05% Triton X-100 for 20 min at room temperature. The cells were incubated with individual primary antibodies for 1 h at room temperature. After washing twice in PBS, the cells were incubated with AlexaFluor™-labeled secondary antibodies (Life Technologies, Carlsbad, USA) for 1 h at room temperature. After washing twice in PBS, the nucleus was counterstained with 4',6-diamidino-2-phenylindole (DAPI). Images were collected with a 60 x water objective lens (NA=1.3) of a confocal laser scanning microscope (Fluoview FV10i) and acquired by using FV10-ASW software (Olympus). For presentation in this manuscript, all images were digitally processed with Adobe Photoshop. Rabbit polyclonal antibodies for human caveolin-1 and human RelA/p65 were purchased from Abcam (Cambridge, UK) and Santa Cruz Biotechnology (Santa Cruz, USA), respectively.

Mouse monoclonal antibody for EBV-encoded EBNA1 and a PE-labeled monoclonal antibody for human leukocyte antigen (HLA)-DR were provided by Drs Hironori Yoshiyama (Hokkaido University and Kenji Oritani (Osaka University), respectively. Rabbit monoclonal antibodies for phophorylated ERK1/2 (The202/Tyr204) and Akt (Ser473) were purchased from Cell signaling technology (Danvers, USA). The percentages of signal-activated cells were analyzed by a confocal laser scanning microscope. Four fields containing approximately 1,000 cells were randomly collected and the fractions of the activated cells were measured.

Flow cytometry

For analysis of FcR expression, Vero-E6 cells (5×10^5) or Akata$^+$ cells (5×10^5) were incubated with αhIgG (1:100) for 1 h on ice. The cells were washed twice in PBS and incubated with FITC-labeled rabbit anti-goat IgG (Sigma-Aldrich, St. Louis, USA) for 30 min on ice. After washing twice in PBS, the binding of αhIgG was analyzed by a flow cytometry. For analysis of the expression of EBV-encoded gp350, Vero-E6 cells were co-cultured with Akata$^-$EBV-eGFP cells in the presence or absence of 0.2% αhIgG. Akata$^-$EBV-eGFP cells were harvested, fixed, permeabilized and blocked as described above. The cells were incubated with anti-gp350 monoclonal antibody (C-1) (44) for 1 h at room temperature, washed twice in PBS,

and incubated with AlexaFluor^{TM} 647-labeled secondary antibodies (Life Technologies). After washing twice in PBS, the expression of gp350 was analyzed by a flow cytometry.

Cell-free EBV infection

Akata^{-}EBV-eGFP cells were treated with 0.2% αhIgG for 48 h for viral production. 1 x 10^5 cells of Vero-E6 cells or Daudi^{-} were incubated with the culture supernatant of αhIgG-treated Akata^{-}EBV-eGFP cells for 1 h at 37˚C. The culture supernatant was replaced with fresh medium and the cells were further incubated for 24 h. The cells were fixed with 4% PFA and the infection efficiencies were analyzed by a flow cytometry as described above.

Inhibitor treatment

Vero-E6 cells were co-cultured with Akata^{-}EBV-eGFP cells and treated with DMSO, U0126 (Sigma-Aldrich), LY294002 hydrochloride (Cell signaling), wortmannin (Sigma-Aldrich) or BAY 11-7082 (Merck, Darmstadt, Germany) for 24 h in the presence or absence of 0.2% αhIgG. U0126, both LY294002 and wortmannin, and BAY11-7082 inhibit the ERK, PI3K, and NF-κB pathways, respectively. Vero-E6 cells were washed and cultured in 6-well plates for 6 h in the absence of αhIgG. The effect of these inhibitors on the transmission of EBV-eGFP into

Vero-E6 cells was analyzed by a flow cytometry as described in EBV transmission assay. The effect of these inhibitors on the expression of gp350 in Akata⁻EBV-eGFP cells was analyzed by flow cytometry as described above.

Knockdown of RelA/p65 by shRNA

Vero-E6 cells (2×10^4) grown in 6-well plates were transfected by FuGENE HG (Roche, Basel, Switzerland) with 3 μg of either pGPU6/GFP/Neo shRNA vectors carrying two identical target sequences against human RelA/p65 subunit of NF-κB (#1:gcccatggaattccagtacct, #2:gaatccagtgtgtgaagaagc) (Shanghai GenePharma, Shanghai, China) or pGPU6/GFP/Neo shRNA control plasmid possessing the target sequence against human glyceraldehyde-3-phosphate dehydrogenase (GAPDH) (gtatgacaacagcctcaag) (Shanghai GenePharma). The individual G418-resistant cell clones were isolated and the down-regulation of RelA/p65 gene was analyzed by RT-PCR with sense (atggacgaactgttc) and antisense (tccttggtgaccaggg) oligonucleotides.

Fluorescent *in situ* hybridization (FISH)

FISH analysis was performed based on the protocol of Nanbo *et al*. (27) with some

modifications. Briefly Akata⁻EBV-eGFP cells were treated with 0.075 M KCl for 20 min at 37ºC, fixed in methanol:acetic acid (3:1) for 30 min at room temperature and spread on the slides. Slides were treated with 4 x SSC (1 x SSC; 0.15 M NaCl, 0.015 M sodium citrate) containing 0.5% (v/v) nonidet P-40 for 30 min at 37ºC, dehydrated in a cold ethanol series (70, 80, 90%) for 2 min each, air dried and denatured in 70% formamide-2 x SSC for 2 min at 72ºC. Slides were dehydrated in a cold ethanol series and air dried. Hybridization probes for detection of EBV plasmids were generated by nick translation using biotin-11-dUTP (Roche). 20 µg of a probe was precipitated by ethanol in the presence of 6 µg salmon sperm DNA (Eppendorf, Hamburg, Germany) and 4 µg human Cot-1 DNA (Life technologies), resuspended in hybridization buffer (2 x SSC, 50% formamide, 10% dextran sulfate) and incubated for 10 min at 70ºC, for 5 min at 4ºC and for 1 h at 37ºC. A hybridization mix containing 5 ng probe was placed on each sample and incubated overnight at 37ºC in a moist chamber. Slides were washed in 2 x SSC containing 50% formamide for 30 min at 50ºC and in 2 x SSC for 30 min at 50ºC. After blocking in 4 x SSC containing 1% BSA, the hybridized probe was revealed by incubation with streptavidin conjugated to Cy3 (Sigma-Aldrich) for 30 min at 37ºC. Slides were washed twice in 4 x SSC containing 0.05% Triton X-100 for 5 min at room temperature. The nucleus was counterstained with DAPI. The percentages of Akata⁻EBV-eGFP cells that underwent the lytic cycle were

analyzed by a confocal laser scanning microscope. Four fields containing approximately 1,000 cells were randomly collected and the fractions of the cells that underwent the lytic cycle were measured.

Results

EBV is transmitted from co-cultured BL cells to epithelial cells.

We established a co-cultivation system to evaluate the efficiency of cell-to-cell EBV transmission. We co-cultured EBV-negative African green monkey kidney epithelial Vero-E6 cells (9, 26) with BL-derived Akata$^-$EBV-eGFP cells, which are latently infected with a recombinant Akata strain EBV encoding eGFP gene inserted into vial genome (22) for 24 h. To amplify the viral transmission, we cross-linked the cell surface IgG of Akata$^-$EBV-eGFP by adding F(ab')$_2$ fragments of goat anti-human IgG polyclonal antibody (αhIgG) to induce the viral lytic cycle (39-41). The transmission of EBV-eGFP to Vero-E6 cells was analyzed by a confocal laser scanning microscope (Fig. 1A and B black bars) and flow cytometry (Fig. 1B gray bars), respectively. EBV-eGFP infected approximately 5% of the cell population by the co-culturing with Akata$^-$EBV-eGFP (Fig. 1A left and middle, and B). αhIgG-treatment increased the transmission rate up to 9% (Fig. 1A right and B).

We also examined the infection efficiency of cell-free virus into Vero-E6 cells. We treated Akata$^-$EBV-eGFP cells with αhIgG for 48 h for the production of EBV-eGFP. Vero-E6 cells or EBV-negative BL-derived Daudi$^-$ (20, 28) were incubated with the culture supernatant of αhIgG-treated Akata$^-$EBV-eGFP cells and the percentages of eGFP-positive cells were analyzed by flow cytometry. The cell-free virus infected Daudi$^-$ cells efficiently (Fig. 1C). In contrast Vero-E6 cells were highly resistant to cell-free viral infection (Fig. 1C).

We also examined the efficiency of EBV transmission into two human gastric epithelial cell lines, such as AGS (2, 49) and NU-GC-3 cell (1, 16, 22, 31, 32, 49). EBV-eGFP was also transmitted to AGS (Fig. 1D, white bars) and NU-GC-3 cells (Fig. 1D, gray bars) in the absence (1.4% and 1.8%, respectively) and in the presence of αhIgG (2.3% and 2.4%, respectively) (Fig. 1D). Because EBV-eGFP was transmitted into Vero-E6 cells more efficiently, we used Vero-E6 cells for further study. We confirmed that eGFP-positive cells expressed an epithelial marker, caveolin-1 (7) (Fig. 1E, left and middle). All eGFP-positive cells expressed EBV-encoded nuclear antigen 1 (EBNA1) (Fig. 1F), indicating that the expressed eGFP in Vero-E6 cells was derived from incoming EBV-eGFP.

Flow cytometric analysis demonstrated that αhIgG bound to the surface of Vero-E6 cells with low efficiency, suggesting that Vero-E6 cells express low levels of Fc receptor (FcR) (Fig.

2A left and B). It is possible that αhIgG-mediated cross-linking of the FcR of Vero-E6 cells initiates cellular signaling pathways and affects viral transmission. A previous study demonstrated that the certain anti-IgG antibodies coat particles of measles virus and enhance viral entry into monocytes and macrophages (14), suggesting that αhIgG-treatment may enhance EBV infection of Vero-E6 cells in a similar way. To test these possibilities, we treated Akata$^-$EBV-eGFP cells with αhIgG for 2 h, replaced the culture medium with fresh medium to remove free αhIgG and co-cultured Akata$^-$EBV-eGFP cells with Vero-E6 cells for an additional 24 h. EBV was transmitted similarly in the presence and absence of free αhIgG (Fig. 2C), indicating that αhIgG-induced enhancement of viral transmission was independent of αhIgG-coated virions and cross-linking of FcR of Vero-E6 cells.

EBV is transmitted from BL cells to epithelial cells *via* cell-to-cell contact

We further examined whether viral transmission requires physical contact. Vero-E6 cells were grown on the basolateral chamber of transculture plates with membrane inserts having pore sizes of 0.4 μm. Akata$^-$EBV-eGFP cells were added to the inserts and incubated for 24 h in the presence or absence of αhIgG. We analyzed the titer of eGFP-EBV in the culture supernatant of the basolateral chamber released from the insert containing αhIgG-treated

Akata$^-$eGFP EBV cells by incubating the culture supernatant with Daudi$^-$ cells. We confirmed that 38% of released eGFP-EBV was transfered to the basolateral chambers through the membrane (data not shown). Viral transmission did not occur if physical cell-to-cell contact was impaired (Fig. 3A left and middle and B), indicating that physical contact is indispensable for efficient viral transmission to epithelial cells.

The EBV lytic cycle induces the expression of the viral glycoproteins, which possess membrane fusion activity (6, 24, 33). To test the possibility that these surface glycoproteins mediate the fusion of plasma membranes between Akata$^-$EBV-eGFP cells and Vero-E6 cells and thus the transfer of virus and/or eGFP to Vero-E6 cells, we assessed the expression of the human leukocyte antigen (HLA)-DR in eGFP-positive Vero-E6 cells by immunofluorescent staining. HLA-DR is the class II histocompatibility molecule constitutively expressed on antigen-presenting cells including B cells, and T lymphocytes only after activation (45). We confirmed that Akata$^-$EBV-eGFP cells expressed HLA-DR and Vero-E6 cells are HLA-DR-negative (Fig. 3C). All eGFP-expressing Vero-E6 cells were HLA-DR-negative (Fig. 3C), indicating that EBV-eGFP transmission was mediated *via* cell-to-cell contact but not *via* cell-to-cell fusion.

The effect of inhibitors of cell signaling pathways on cell-to-cell contact-mediated EBV transmission

Because the molecular mechanism of cell-to-cell EBV transmission remains undefined, we investigated the roles of cellular signaling pathways in this process by using specific inhibitors. We co-cultured Vero-E6 cells with Akata⁻EBV-eGFP cells in the presence and absence of αhIgG under the treatment of inhibitors, such as U0126, LY294002, wortmannin or BAY11-7082. U0126, both LY294002 and wortmannin, and BAY11-7082 inhibit the ERK (11), PI3K (46), and NF-κB pathways (50), respectively. We treated the cells with these inhibitors in various concentrations that didn't exhibit cytotoxicity. αhIgG-treatment triggers a variety of signaling pathways concurrent with induction of the lytic cycle (36). To exclude the possibility that the inhibitors reduced αhIgG-induced viral production, we also measured the effect of these inhibitors on the expression of viral lytic gene, gp350 (22, 30) by flow cytometric analysis. The expression of gp350 was enhanced under the treatment of αhIgG (Fig. 4A bottom). U0126 and BAY11-7082 significantly inhibited cell-to-cell contact-mediated EBV transmission (Fig. 4A top) with a moderate impairment of gp350 expression (Fig. 4A bottom), suggesting that the ERK and the NF-κB pathways appear to contribute to EBV transmission in addition to lytic induction. Both PI3K inhibitors, LY294002 and wortmannin, blocked EBV

transmission and gp350 expression similarly (Fig. 4A), suggesting that blockage of PI3K pathway impaired EBV transmission coupled with inhibition of the lytic induction.

We further examined the role of the NF-κB pathway in cell-to-cell contact-mediated EBV transmission by using short hairpin RNAs (shRNA) targeting RelA/p65 subunit of NF-κB in Vero-E6 cells (Fig. 4B). The knockdown of RelA/p65 significantly reduced viral transmission (Fig. 4C). Taken together, the NF-κB pathway contributes to EBV transmission and moderately to the viral lytic cycle. The inhibitor treatments and knockdown of RelA/p65 also reduced viral transmission and lytic induction in the absence of αhIgG (Fig. 4A and C).

Cell signaling molecules activate immediately in the co-cultivated cells.

Because specific inhibitors of the ERK, PI3K, and NF-κB pathways significantly blocked cell-to-cell contact-mediated EBV transmission, we examined whether these signaling molecules are activated in co-cultured BL cells and epithelial cells. We assessed the status of the ERK, PI3K and NF-κB signaling pathways by immunofluorescent staining in Akata$^-$EBV-eGFP cells and Vero-E6 cells, respectively. By using a laser-scanning confocal microscope, we confirmed that the individual marker proteins in Akata$^-$EBV-eGFP cells (HLA-DR) or Vero-E6 cells (caveolin-1) were detected without leak of the signal derived from

co-cultured cells (Fig. 5A).

Under stimulation of the ERK pathway, the activation loop residues, Thr202/Tyr204 and Thr185/Tyr187 of ERK are phosphorylated by a sequential protein kinase cascade (3). We analyzed the phosphorylation status of ERK by immunofluorescent staining. Phosphorylated ERK was observed diffusely in the cytoplasm in both Akata$^-$EBV-eGFP cells (Fig. 5B and D) and Vero-E6 cells (Fig. 5C and D) 30 min after co-cultivation. The phosphorylation was transient and disappeared 1 h after co-cultivation in both Akata$^-$EBV-eGFP cells and Vero-E6 cells (Fig. 5B-D).

To analyze the activation of the PI3K pathway, we assessed the level of phospho-Ser473 of Akt, which is a key component of the pathway (21). The phosphorylated Akt was distributed in the plasma membrane of Akata$^-$EBV-eGFP cells 1 h after co-cultivation and the activation stably continued (Fig. 6A and C). Akt was transiently phosphorylated in the cytoplasm of Vero-E6 cells 1 h after co-cultivation (Fig. 6B and C).

Following stimulation of the NF-κB pathway, the IKB inhibitory subunit of the NF-κB complex is phosphorylated, ubiquitinated and degraded and the transcription factor subunits of the NF-κB complex subunit (RelA/p65 and p50) translocate into the nucleus, resulting in the modulation of gene transcription (23). Because its nuclear import is a key event in NF-κB

activation, we assessed the distribution of the RelA/p65 subunit in co-cultured cells by immunofluorescent staining. RelA/p65 transiently translocated to the nucleus in co-cultured Vero-E6 cells (Fig. 7B and C). In contrast, RelA/p65 translocated to the nucleus in Akata$^-$EBV-eGFP cells 24 h after co-cultivation (Fig. 7A and C). The treatments of U0126, LY294002, wortmannin or BAY11-7082 specifically blocked the activation of individual target molecules (Fig. 5-7). Interestingly these signaling molecules were also activated in the co-cultured cells in the absence of αhIgG (Fig. 5-7).

Cell-to-cell contact induces viral replication.

We observed that EBV is transmitted to epithelial cells in the absence of αhIgG (Fig. 1A-C). The inhibitor treatments and the knockdown of RelA/p65 also reduced viral transmission and lytic induction in the absence of αhIgG (Fig. 4A and C). The signaling molecules were activated in the co-cultured cells in the absence of αhIgG (Fig. 5A and 6A). Therefore we tested whether cell-to-cell contact induces the viral lytic cycle in the latently infected Akata$^-$EBV-eGFP cells and leads to the viral transmission. We co-cultured Vero-E6 cells with Akata$^-$EBV-eGFP cells and analyzed the efficiencies of lytic induction in Akata$^-$EBV-eGFP cells by FISH analyses using Cy3-labeled probe, which specifically hybridized

to EBV genome. The EBV genomes were significantly amplified (10^2 to 10^3 fold) in the nucleus under the treatment of αhIgG (Fig. 8A bottom, right). FISH analysis showed that less than 1% of the cell population underwent lytic without αhIgG-treatment (Fig. 8A top left, and B). By αhIgG treatment 12% of Akata$^-$EBV-eGFP cells underwent the lytic cycle (Fig. 8A top middle, and B). The rate of lytic induction in Akata$^-$EBV-eGFP cells increased up to 2% by co-cultivation with Vero-E6 cells (Fig 8A top right, and B), indicating that cell-to-cell contact between EBV-latently infected BL with epithelial cells initiated lytic induction. Immunofluorescent staining analysis also demonstrated that gp350 expression was enhanced in Akata$^-$EBV-eGFP cells by co-cultivation with Vero-E6 cells (Fig. 8C).

Discussion

In our present study, we demonstrated the roles of the cell signaling pathways in cell-to-cell contact-mediated EBV transmission by using an *in vitro* co-cultivation system. Our observations indicate that; (i) cell-to-cell contact without cell-to-cell fusion contributes to viral transmission (Fig. 1-3); (ii) the treatment of inhibitors of the ERK and NF-κB pathways down-regulates EBV transmission in addition to lytic induction; blockage of the PI3K pathway impairs EBV transmission coupled with inhibition of the lytic induction; knockdown of RelA/p65

significantly down-regulates cell-to-cell contact-mediated viral transmission (Fig. 4); (iii) the ERK, PI3K and NF-κB pathways are activated in co-cultured BL and epithelial cells (Fig. 5-7); (iiii) cell-to-cell contact initiates induction of the lytic cycle in BL cells (Fig. 8).

αhIgG-treatment amplified EBV transmission into epithelial cells (Fig. 1A, B and D), indicating that the synthesis of progeny virus in Akata$^-$EBV-eGFP cells is indispensable for cell-to-cell viral transmission. It has been reported that a small fraction of Akata cells (1%) spontaneously enters into the lytic cycle (41) (Fig. 8A left). By co-cultivation with Vero-E6 cells, the vial lytic cycle was induced in Akata$^-$EBV-eGFP cells (Fig. 8A middle and B) in the absence of αhIgG, suggesting the cell-to-cell contact-mediated lytic induction contributes to the viral transmission into the epithelial cells under physiological conditions. It has been shown that a variety of signal transductions including the ERK and PI3K pathways are synergistically activated during EBV lytic cycle (18). We showed that the specific inhibitors of the ERK and PI3K pathways blocked EBV replication (Fig. 4A, bottom) and that ERK and Akt were phosphorylated in co-cultured Akata$^-$EBV-eGFP cells in the absence of αhIgG-treatment (Fig. 5 and 6). These data suggest that the activation of the ERK and PI3K pathways contribute to cell-to-cell contact-mediated viral lytic induction in Akata$^-$EBV-eGFP cells. It is known that the EBV-encoded immediate early protein ZTA, which is important for the switch to viral lytic

replication, is inhibited by the RelA/p65 subunit (4, 25). However, no enhancement of EBV replication was observed under BAY11-7082 treatment in our study (Fig. 4 bottom). The discrepancy may result from a difference in the experimental systems (e.g. single cultured B cells versus co-cultured B cells). The NF-κB pathway was activated in Akata$^-$EBV-eGFP cells in the late stage of cell-to-cell contact-mediated EBV transmission (Fig. 7A and C). The role of the NF-κB pathway in B cells in cell-to-cell contact-mediated EBV transmission remains unclear and its further investigation is required.

Shannon-Lowe and colleagues have demonstrated that EBV virions loaded on the surface of primary B cells facilitate the formation of a virological synapse (VS)-like intercellular conjugation between B cells and co-cultured epithelial cells (34, 35). The VS is a tight adhesive junction across which virus can be efficiently transferred from virus-infected cells to non-infected target cells without cell-cell fusion. The VS has been intensively studied in the field of retroviruses (17). The ERK pathway appears to enhance the polarization of the mitotic organizing center (MTOC) and contributes to microtubule-dependent trafficking of viral gag proteins (29). We demonstrated that an ERK inhibitor, U0126 significantly blocked EBV transmission with a partial impairment of induction of the lytic cycle (Fig. 4A) and that the ERK was phosphorylated in co-cultured Akata$^-$EBV-eGFP cells (Fig. 5A). These observations

suggest that the ERK pathway likely plays a role in the efficient trafficking of EBV virions to the intercellular space mediated by MTOC polarization.

We also demonstrated that the PI3K and NF-κB pathways contribute to viral transmission (Fig. 4). Previous observations have demonstrated an important role of an EBV glycoprotein, BMRF-2 in the cell-to-cell spread of EBV in polarized oral epithelial cells (47, 48). BMRF-2 interacts with β1 and αv integrins and initiates PI3K signaling, events crucial for EBV's entry into B cells (10). NF-κB signaling is activated by the conjugation of viral gp350/200 with CD21 in B cells (8, 38). It is possible that both binding of BMRF-2 to the integrins and that of gp350/200 to undefined viral receptors in epithelial cells trigger the PI3K and NF-κB pathways and promote entry of intercellular EBV virions into adjacent epithelial cells. We demonstrated that the phosphorylation of Akt and the nuclear translocation of RelA/p65 were induced in Vero-E6 cells 1 h after co-cultivation (Fig. 6B and C). The expression of viral glycoproteins and the generation of progeny virions are unlikely to be induced in 1 h after cell-to-cell contact-mediated lytic induction. The roles of the PI3K and NF-κB in the processes of EBV's entry into epithelial cells mediated by cell-to-cell contact currently remain unknown and warrant further investigation.

In our study we used a monkey and two human epithelial cell lines as recipient cells. It

would be interesting and informative to test our findings in EBV-negative primary human epithelial cells in the future.

Taken together, this study provides a tractable system to examine cell-to-cell transmission of EBV to epithelial cells. Our observations indicate that multiple intracellular signaling molecules play roles in cell-to-cell contact-mediated EBV transmission, and serve as a basis to understand better the mechanism of cell-to-cell viral transmission.

Acknowledgement

We acknowledge Drs Ayato Takada (Hokkaido University), Kenji Oritani (Osaka University), and Hironori Yoshiyama for providing us with Vero-E6 cells, PE-labeled anti-human HLA-DR antibody, and anti-EBNA1 polyclonal antibody, respectively. We also thank Drs Bill Sugden (University of Wisconsin, Madison) and Yusuke Ohba (Hokkaido University) for critically reviewing the manuscript. This work was supported by grants-in-aid from the Japanese Ministry of Education, Science, Sports, Culture, and Technology, Japan.

References

1. **Akiyama, S., H. Amo, T. Watanabe, M. Matsuyama, J. Sakamoto, M. Imaizumi, H. Ichihashi, T. Kondo, and H. Takagi.** 1988. Characteristics of three human gastric cancer cell lines, NU-GC-2, NU-GC-3 and NU-GC-4. Jpn J Surg **18:**438-46.

2. **Barranco, S. C., C. M. Townsend, Jr., C. Casartelli, B. G. Macik, N. L. Burger, W. R. Boerwinkle, and W. K. Gourley.** 1983. Establishment and characterization of an in vitro model system for human adenocarcinoma of the stomach. Cancer Res **43:**1703-9.

3. **Boulton, T. G., S. H. Nye, D. J. Robbins, N. Y. Ip, E. Radziejewska, S. D. Morgenbesser, R. A. DePinho, N. Panayotatos, M. H. Cobb, and G. D. Yancopoulos.** 1991. ERKs: a family of protein-serine/threonine kinases that are activated and tyrosine phosphorylated in response to insulin and NGF. Cell **65:**663-75.

4. **Brown, H. J., M. J. Song, H. Deng, T. T. Wu, G. Cheng, and R. Sun.** 2003. NF-kappaB inhibits gammaherpesvirus lytic replication. J Virol **77:**8532-40.

5. **Chang, Y., C. H. Tung, Y. T. Huang, J. Lu, J. Y. Chen, and C. H. Tsai.** 1999. Requirement for cell-to-cell contact in Epstein-Barr virus infection of nasopharyngeal carcinoma cells and keratinocytes. J Virol **73:**8857-66.

6. **Connolly, S. A., J. O. Jackson, T. S. Jardetzky, and R. Longnecker.** 2011. Fusing structure and function: a structural view of the herpesvirus entry machinery. Nat Rev Microbiol **9:**369-81.

7. **Couet, J., M. M. Belanger, E. Roussel, and M. C. Drolet.** 2001. Cell biology of caveolae and caveolin. Adv Drug Deliv Rev **49:**223-35.

8. **de Oliveira, D. E., G. Ballon, and E. Cesarman.** 2010. NF-kappaB signaling modulation by EBV and KSHV. Trends Microbiol **18:**248-57.

9. **Desmyter, J., J. L. Melnick, and W. E. Rawls.** 1968. Defectiveness of interferon production and of rubella virus interference in a line of African green monkey kidney cells (Vero). J Virol **2:**955-61.

10. **Dorner, M., F. Zucol, D. Alessi, S. K. Haerle, W. Bossart, M. Weber, R. Byland, M. Bernasconi, C. Berger, S. Tugizov, R. F. Speck, and D. Nadal.** 2010. beta1 integrin expression increases susceptibility of memory B cells to Epstein-Barr virus infection. J Virol **84:**6667-77.

11. **Favata, M. F., K. Y. Horiuchi, E. J. Manos, A. J. Daulerio, D. A. Stradley, W. S. Feeser, D. E. Van Dyk, W. J. Pitts, R. A. Earl, F. Hobbs, R. A. Copeland, R. L. Magolda, P. A. Scherle, and J. M. Trzaskos.** 1998. Identification of a novel inhibitor of mitogen-activated protein kinase kinase. J Biol Chem **273:**18623-32.

12. **Fingeroth, J. D., M. E. Diamond, D. R. Sage, J. Hayman, and J. L. Yates.** 1999. CD21-Dependent infection of an epithelial cell line, 293, by Epstein-Barr virus. J Virol **73:**2115-25.

13. **Hutt-Fletcher, L. M.** 2007. Epstein-Barr virus entry. J Virol **81:**7825-32.

14. **Iankov, I. D., M. Pandey, M. Harvey, G. E. Griesmann, M. J. Federspiel, and S. J. Russell.** 2006. Immunoglobulin g antibody-mediated enhancement of measles virus infection can bypass the protective antiviral immune response. J Virol **80:**8530-40.

15. **Imai, S., J. Nishikawa, and K. Takada.** 1998. Cell-to-cell contact as an efficient mode of Epstein-Barr virus infection of diverse human epithelial cells. J Virol **72:**4371-8.

16. **Iwakiri, D., Y. Eizuru, M. Tokunaga, and K. Takada.** 2003. Autocrine growth of Epstein-Barr virus-positive gastric carcinoma cells mediated by an Epstein-Barr virus-encoded small RNA. Cancer Res **63:**7062-7.

17. **Jolly, C., and Q. J. Sattentau.** 2004. Retroviral spread by induction of virological synapses. Traffic **5:**643-50.

18. **Kenney, S. C.** 2007. Reactivation and lytic replication of EBV.

19. **Kieff, E., and A. B. Rickinson.** 2001. Epstein-Barr virus and its replication. In M. Knipe and P. M. Howley (ed.), Fields virology, 4th ed. Lippincott Williams & Wilkins, Philadelphia, PA**:**2511-73.

20. **Klein, E., G. Klein, J. S. Nadkarni, J. J. Nadkarni, H. Wigzell, and P. Clifford.** 1968. Surface IgM-kappa specificity on a Burkitt lymphoma cell in vivo and in derived culture lines. Cancer Res **28:**1300-10.

21. **Liu, P., H. Cheng, T. M. Roberts, and J. J. Zhao.** 2009. Targeting the phosphoinositide 3-kinase pathway in cancer. Nat Rev Drug Discov **8:**627-44.

22. **Maruo, S., L. Yang, and K. Takada.** 2001. Roles of Epstein-Barr virus glycoproteins gp350 and gp25 in the infection of human epithelial cells. J Gen Virol **82:**2373-83.

23. **Mattioli, I., A. Sebald, C. Bucher, R. P. Charles, H. Nakano, T. Doi, M. Kracht, and M. L. Schmitz.** 2004. Transient and selective NF-kappa B p65 serine 536 phosphorylation induced by T cell costimulation is mediated by I kappa B kinase beta and controls the kinetics of p65 nuclear import. J Immunol **172:**6336-44.

24. **McShane, M. P., and R. Longnecker.** 2004. Cell-surface expression of a mutated Epstein-Barr virus glycoprotein B allows fusion independent of other viral proteins. Proc Natl Acad Sci U S A **101:**17474-9.

25. **Mothes, W., N. M. Sherer, J. Jin, and P. Zhong.** 2010. Virus cell-to-cell transmission. J Virol **84:**8360-8.

26. **Nanbo, A., M. Imai, S. Watanabe, T. Noda, K. Takahashi, G. Neumann, P. Halfmann, and Y. Kawaoka.** 2010. Ebolavirus is internalized into host cells via macropinocytosis in a viral glycoprotein-dependent manner. PLoS Pathog **6:**e1001121.

27. **Nanbo, A., A. Sugden, and B. Sugden.** 2007. The coupling of synthesis and partitioning of EBV's plasmid replicon is revealed in live cells. EMBO J **26:**4252-62.

28. **Nanbo, A., H. Yoshiyama, and K. Takada.** 2005. Epstein-Barr virus-encoded poly(A)-RNA confers resistance to apoptosis mediated through Fas by blocking the PKR pathway in human epithelial intestine 407 cells. J Virol **79:**12280-5.

29. **Nejmeddine, M., V. S. Negi, S. Mukherjee, Y. Tanaka, K. Orth, G. P. Taylor, and C. R. Bangham.** 2009. HTLV-1-Tax and ICAM-1 act on T-cell signal pathways to polarize the microtubule-organizing center at the virological synapse. Blood **114:**1016-25.

30. **Nemerow, G. R., C. Mold, V. K. Schwend, V. Tollefson, and N. R. Cooper.** 1987. Identification of gp350 as the viral glycoprotein mediating attachment of Epstein-Barr virus (EBV) to the EBV/C3d receptor of B cells: sequence homology of gp350 and C3 complement fragment C3d. J Virol **61:**1416-20.

31. **Nishikawa, J., S. Imai, T. Oda, T. Kojima, K. Okita, and K. Takada.** 1999. Epstein-Barr virus promotes epithelial cell growth in the absence of EBNA2 and LMP1 expression. J Virol **73:**1286-92.

32. **Oda, T., S. Imai, S. Chiba, and K. Takada.** 2000. Epstein-Barr virus lacking glycoprotein gp85 cannot infect B cells and epithelial cells. Virology **276:**52-8.

33. **Omerovic, J., L. Lev, and R. Longnecker.** 2005. The amino terminus of Epstein-Barr virus glycoprotein gH is important for fusion with epithelial and B cells. J Virol **79:**12408-15.

34. **Shannon-Lowe, C., and M. Rowe.** 2011. Epstein-Barr virus infection of polarized epithelial cells via the basolateral surface by memory B cell-mediated transfer infection. PLoS Pathog **7:**e1001338.

35. **Shannon-Lowe, C. D., B. Neuhierl, G. Baldwin, A. B. Rickinson, and H. J. Delecluse.** 2006. Resting B cells as a transfer vehicle for Epstein-Barr virus infection of epithelial cells. Proc Natl Acad Sci U S A **103:**7065-70.

36. **Sinclair, A. J., and P. J. Farrell.** 1995. Host cell requirements for efficient infection of quiescent primary B lymphocytes by Epstein-Barr virus. J Virol **69:**5461-8.

37. **Speck, P., and R. Longnecker.** 2000. Infection of breast epithelial cells with Epstein-Barr virus via cell-to-cell contact. J Natl Cancer Inst **92:**1849-51.

38. **Sugano, N., W. Chen, M. L. Roberts, and N. R. Cooper.** 1997. Epstein-Barr virus binding to CD21 activates the initial viral promoter via NF-kappaB induction. J Exp Med **186:**731-7.

39. **Takada, K.** 1984. Cross-linking of cell surface immunoglobulins induces Epstein-Barr virus in Burkitt lymphoma lines. Int J Cancer **33:**27-32.

40. **Takada, K., K. Horinouchi, Y. Ono, T. Aya, T. Osato, M. Takahashi, and S. Hayasaka.** 1991. An Epstein-Barr virus-producer line Akata: establishment of the cell line and analysis of viral DNA. Virus Genes **5:**147-56.

41. **Takada, K., and Y. Ono.** 1989. Synchronous and sequential activation of latently infected Epstein-Barr virus genomes. J Virol **63:**445-9.

42. **Tao, Q., G. Srivastava, A. C. Chan, L. P. Chung, S. L. Loke, and F. C. Ho.** 1995. Evidence for lytic infection by Epstein-Barr virus in mucosal lymphocytes instead of nasopharyngeal epithelial cells in normal individuals. J Med Virol **45:**71-7.

43. **Tao, Q., G. Srivastava, A. C. Chan, and F. C. Ho.** 1995. Epstein-Barr-virus-infected nasopharyngeal intraepithelial lymphocytes. Lancet **345:**1309-10.

44. **Thorley-Lawson, D. A., and K. Geilinger.** 1980. Monoclonal antibodies against the major glycoprotein (gp350/220) of Epstein-Barr virus neutralize infectivity. Proc Natl Acad Sci U S A **77:**5307-11.

45. **Trowsdale, J., J. Ragoussis, and R. D. Campbell.** 1991. Map of the human MHC. Immunol Today **12:**443-6.

46. **Walker, E. H., M. E. Pacold, O. Perisic, L. Stephens, P. T. Hawkins, M. P. Wymann, and R. L. Williams.** 2000. Structural determinants of phosphoinositide 3-kinase

inhibition by wortmannin, LY294002, quercetin, myricetin, and staurosporine. Mol Cell **6:**909-19.

47. **Xiao, J., J. M. Palefsky, R. Herrera, J. Berline, and S. M. Tugizov.** 2009. EBV BMRF-2 facilitates cell-to-cell spread of virus within polarized oral epithelial cells. Virology **388:**335-43.

48. **Xiao, J., J. M. Palefsky, R. Herrera, J. Berline, and S. M. Tugizov.** 2008. The Epstein-Barr virus BMRF-2 protein facilitates virus attachment to oral epithelial cells. Virology **370:**430-42.

49. **Yoshiyama, H., S. Imai, N. Shimizu, and K. Takada.** 1997. Epstein-Barr virus infection of human gastric carcinoma cells: implication of the existence of a new virus receptor different from CD21. J Virol **71:**5688-91.

50. **Zanotto-Filho, A., A. Delgado-Canedo, R. Schroder, M. Becker, F. Klamt, and J. C. Moreira.** 2010. The pharmacological NFkappaB inhibitors BAY117082 and MG132 induce cell arrest and apoptosis in leukemia cells through ROS-mitochondria pathway activation. Cancer Lett **288:**192-203.

Figure Legends

Fig. 1. EBV is transmitted from BL cells to epithelial cells by co-cultivation.

(A) EBV transmission from BL cells to epithelial cells is facilitated by αhIgG treatment. Vero-E6 cells were co-cultured with Akata$^-$EBV-eGFP cells in the absence (middle panel) or presence (right panel) of αhIgG for 24 h. The infection of EBV-eGFP in Vero-E6 cells (green) was analyzed by a confocal laser scanning microscope. The left panel shows the result without co-cultivation. The nucleus was counterstained with DAPI. Scale bars, 100 μm. (B) A summary of cell-to-cell contact-mediated EBV transmission. Vero-E6 cells were co-cultured with Akata$^-$EBV-eGFP cells in the absence or presence of αhIgG for 24 h. The percentages of EBV-eGFP-positive Vero-E6 cells were analyzed by a confocal laser scanning microscope (black bars) or flow cytometry (gray bars). The experiment was performed five times independently and the average and its standard deviation are shown in each condition. *, $P < 0.05$ versus respective control (Student's *t* test). (C) Infection of cell-free EBV-eGFP into Vero-E6 cells. Vero-E6 cells or Daudi$^-$ cells were incubated for 1 h at 37˚C with culture supernatants derived from αhIgG-treated (gray bars) or -untreated (black bars) Akata$^-$EBV-eGFP cells. The culture supernatants were replaced with fresh medium and the cells were further incubated for 48 h.

The percentages of eGFP-positive cells were analyzed by flow cytometry. The experiment was performed three times independently. The average and its standard deviation are shown in each condition. **, $P < 0.01$ versus respective control (Student's *t* test). (D) EBV-eGFP is transmitted to human gastric epithelial cells. AGS (white bars), NU-GC-3 (gray bars) or Vero-E6 cells (black bars) were co-cultured with Akata$^-$EBV-eGFP cells in the absence or presence of αhIgG for 24 h. The percentages of eGFP-positive epithelial cells were analyzed by flow cytometry. The experiment was performed three times independently and the average and its standard deviation are shown in each condition. *, $P < 0.05$ versus respective control. **, $P < 0.01$ versus respective control (Student's *t* test). (E) EBV-eGFP is transmitted to Vero-E6 cells. Vero-E6 cells were co-cultured with Akata$^-$EBV-eGFP cells under the treatment of αhIgG for 24 h. The expression of an epithelium marker, caveolin-1 was analyzed by immunofluorescent staining. Caveolin-1 (red, middle) was expressed in eGFP-positive cells (green, left). BL-derived Akata$^-$EBV-eGFP cells were caveolin-1-negative (right). The nucleus was counterstained with DAPI. Scale bars, 20 μm. (F) eGFP-positive Vero-E6 cells are infected with EBV-eGFP. Vero-E6 cells were co-cultured with Akata$^-$EBV-eGFP cells under the treatment of αhIgG for 24 h. The expression of EBV-encoded nuclear antigen 1 (EBNA1) was analyzed by immunofluorescent staining. eGFP-positive Vero-E6 cells (green, left) were

EBNA1-positive (red, right). The nucleus was counterstained with DAPI. Scale bars, 20 μm.

Fig. 2. The role of free αhIgG in viral transmission.

(A) The binding of αhIgG to Vero-E6. Vero-E6 cells (left) or Akata^{+} cells (right) were incubated with 0.1% αhIgG on ice. The binding of αhIgG was revealed with FITC-labeled secondary antibody (bold lines) by flow cytometry. As control the cells were incubated with the secondary antibody (thin lines). (B) Summary of binding of αhIgG. The efficiency of binding of αhIgG to Vero-E6 or Akata^{+} cells was quantified by flow cytometry (black bars). As control the cells were incubated with the secondary antibody (gray bars). The experiment was performed three times independently and the average and its standard deviation are shown in each condition. **, $P < 0.01$ versus respective control (Student's *t* test). (C) The role of free αhIgG in viral transmission. Akata^{-}EBV-eGFP cells were treated with αhIgG for 2 h, washed to remove free αhIgG, and co-cultured with Vero-E6 cells for 24 h. The percentage of eGFP-positive epithelial cells was analyzed by flow cytometry. As control Akata^{-}EBV-eGFP cells were co-cultured with Vero-E6 cells in the presence of free αhIgG. The experiment was performed three times independently and the average and its standard deviation are shown in each condition. **, $P < 0.01$ versus respective control (Student's *t* test).

Fig. 3. EBV is transmitted from BL cells to epithelial cells *via* cell-to-cell contact.

(A) Physical cell-to-cell contact requires for EBV transmission. Vero-E6 cells were grown in the basolateral chamber of transculture inserts with pore sizes of 0.4 μm. Akata$^-$EBV-eGFP was added to the inserts and incubated in the presence (left) or absence (middle) of αhIgG for 24 h. As control Vero-E6 cells were co-cultured with Akata$^-$EBV-eGFP in the presence of αhIgG (right). The infection of EBV-eGFP into Vero-E6 (green) was analyzed by a confocal laser scanning microscope. The nucleus was counterstained with DAPI. Scale bars, 100 μm. (B) A summary of viral transmission with physical barrier. Vero-E6 cells were grown in the basolateral chamber of transculture plates. Akata$^-$EBV-eGFP cells were added to the inserts and incubated in the presence (gray bars) or absence (black bars) of αhIgG for 24 h. As control Vero-E6 cells were co-cultured with Akata$^-$EBV-eGFP in the presence (gray bars) or absence (black bars) of αhIgG. The infection of EBV-eGFP in Vero-E6 was analyzed by flow cytometry. The experiment was performed three times independently. The average and its standard deviation are shown in each condition. **, $P < 0.01$ versus respective control (Student's *t* test). (C) EBV transmits from BL cells to epithelial cells *via* cell-to-cell contact. Akata$^-$EBV-eGFP cells were co-cultured with Vero-E6 cells in the presence of αhIgG for 24 h. The expression of

HLA-DR (red) in Akata⁻EBV-eGFP or Vero-E6 cells was analyzed by immunofluorescent staining (left panels). HLA-DR (red) was expressed in eGFP-positive Vero-E6 cells (green) (right panels). The nucleus was counterstained with DAPI. Scale bars, 20 μm.

Fig. 4. The effect of the inhibitors of cell signaling pathways on cell-to-cell contact-mediated EBV transmission and replication.

(A) The effect of the inhibitors on cell-to-cell contact-mediated EBV transmission (top) and EBV replication (bottom). Vero-E6 were co-cultured with Akata⁻EBV-eGFP cells in the presence (gray bars) or absence (black bars) of αhIgG under the treatment of DMSO, U0126, LY294002, wortmannin or BAY11-7082 for 24 h. The percentages of eGFP-positive cells were analyzed by flow cytometry. The data were normalized to αhIgG-untreated and DMSO-treated cells (top). Co-cultured Akata⁻EBV-eGFP cells were harvested and the expression of gp350 was analyzed by flow cytometry. The data were normalized to αhIgG-untreated and DMSO-treated cells (bottom). The experiment was performed three times independently. The average and its standard deviation are shown in each condition. (B) RelA/p65 knockdown by shRNA in Vero-E6 cells. Total RNA was isolated from two Vero-E6 clones stably expressing shRNA against human NF-κB RelA/p65 (RelA/p65-shRNA #1 and #2), and control expressing shRNA

against human GAPDH (GAPDH-shRNA). Knock down of RelA/p65 mRNA was analyzed by RT-PCR (top). As control the expression of β-actin mRNA is shown (bottom). (C) The effect of RelA/p65 knockdown on cell-to-cell contact-mediated EBV transmission. RelA/p65-shRNA or GAPDH-shRNA were co-cultured with Akata$^-$EBV-eGFP cells in the presence (gray bars) or absence (black bars) of αhIgG for 24 h. Viral transmission was assessed by flow cytometry. The experiment was performed three times independently. The average and its standard deviation are shown in each condition. **, $P < 0.01$ versus respective control (Student's *t* test).

Fig. 5. The activation of the ERK pathway in co-cultured cells.

(A) Immunofluorescent staining analysis in co-culture cells. Vero-E6 cells grown in 35 mm glass-bottomed culture dishes were co-cultured with Akata$^-$EBV-eGFP cells for 4 h. The cells were harvested and subjected to immunofluorescent staining to analyze the expressions of HLA-DR in Akata$^-$EBV-eGFP cells (top, left) or caveolin-1 in Vero-E6 cells (bottom, middle) in co-cultured condition. The bright field images are shown (right). Scale bars, 100 μm. ERK is phosphorylated in co-cultured Akata$^-$EBV-eGFP (B) or Vero-E6 cells (C). Vero-E6 cells were co-cultured with Akata$^-$EBV-eGFP cells in the presence (b-e) or absence (f) of αhIgG for various times. The phosphorylation of ERK in Akata$^-$EBV-eGFP (B) or Vero-E6 cells (C) was

examined by immunofluorescent staining (top). The effect of U0126 treatment (0.2 μM) on the phosphorylation of ERK is shown in (e). As control the status of ERK phosphorylation in αhIgG-untreated Akata$^-$EBV-eGFP or Vero-E6 cells is shown in (a). Bright field images are shown (bottom). Scale bars, 100 μm. (D) The percentages of the cells contain the phosphorylation of ERK were analyzed by a confocal laser scanning microscope. The experiment was performed three times independently. The average and its standard deviation are shown in each condition. **, $P < 0.01$ versus respective control (Student's *t* test).

Fig. 6. The activation of the PI3K pathway in co-cultured cells.

Akt is phosphorylated in co-cultured Akata$^-$EBV-eGFP (A) or Vero-E6 cells (B). Vero-E6 cells were co-cultured with Akata$^-$EBV-eGFP cells in the presence (b-f) or absence (g) of αhIgG for various times. The phosphorylation of Akt in Akata$^-$EBV-eGFP (A) or Vero-E6 cells (B) was examined by immunofluorescent staining (top). The effect of LY294002 treatment (0.2 μM) (e) or wortmannin treatment (0.1 μM) (f) on the phosphorylation of Akt is shown. As control the status of Akt phosphorylation in αhIgG-untreated Akata$^-$EBV-eGFP or Vero-E6 cells is shown in (a). Bright field images are shown (bottom). Scale bars, 100 μm. (C) The percentages of the cells exhibiting phosphorylation of Akt were analyzed by a confocal laser scanning microscope.

The experiment was performed three times independently. The average and its standard deviation are shown in each condition. **, $P < 0.01$ versus respective control (Student's *t* test).

Fig. 7. The activation of the NF-κB pathway in co-cultured cells.

The nuclear translocation of RelA/p65 in co-cultured Akata$^-$EBV-eGFP (A) or Vero-E6 cells (B). Vero-E6 cells were co-cultured with Akata$^-$EBV-eGFP cells in the presence (b-e) or absence (f) of αhIgG for various times. The translocation of RelA/p65 in Akata$^-$EBV-eGFP (A) or Vero-E6 cells (B) was examined by immunofluorescent staining (top). The effect of BAY11-7082 treatment (2 μM) on the translocation of RelA/p65 is shown in (e). As control the status of RelA/p65 translocation in αhIgG-untreated Akata$^-$EBV-eGFP or Vero-E6 cells is shown in (a). The nucleus is counterstained with DAPI (bottom). Insets show enlargements of the boxed areas. Scale bars, 100 μm. (C) The percentages of the cells that contain the translocation of RelA/p65 were analyzed by a confocal laser scanning microscope. The experiment was performed three times independently. The average and its standard deviation are shown in each condition. **, $P < 0.01$ versus respective control (Student's *t* test).

Fig. 8. Lytic cycle is induced in co-cultured BL cells.

(A) Vero-E6 cells were co-cultured with Akata$^-$EBV-eGFP cells in the absence of αhIgG for 24 h (top, right). As control Akata$^-$EBV-eGFP cells were treated in the presence (top, middle) or absence of αhIgG (top, left). Akata$^-$EBV-eGFP cells were harvested and induction of the lytic cycle was analyzed by FISH using Cy3-labeled probe for EBV genome (top). Enlarged images of the cell in latent (bottom, left) or lytic (bottom, right) phase are shown. The nucleus was counterstained with DAPI. Scale bars:100 μm. (B) The percentages of Akata$^-$EBV-eGFP cells undergoing the lytic cycle were analyzed by a confocal laser scanning microscope. The experiment was performed three times independently. The average and its standard deviation are shown in each condition. **, $P < 0.01$ versus respective control (Student's *t* test). (C) The expression of gp350 in co-cultured BL cells. The expression of gp350 was analyzed by flow cytometry. The experiment was performed three times independently. The average and its standard deviation are shown in each condition. **, $P < 0.01$ versus respective control (Student's *t* test).

Fig. 1

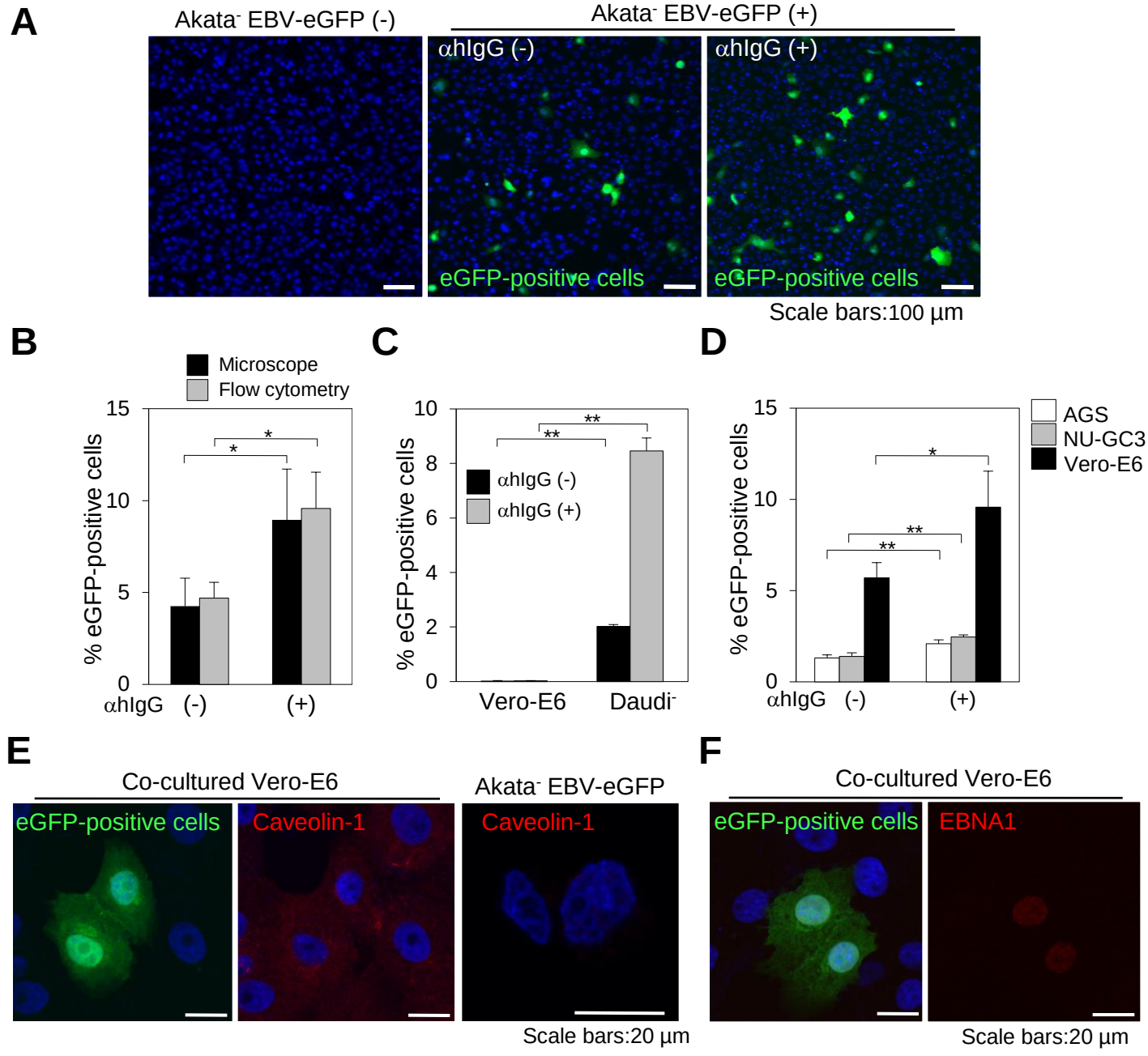
A
Akata- EBV-eGFP (-)
Akata- EBV-eGFP (+)
αhIgG (-)
αhIgG (+)
eGFP-positive cells
eGFP-positive cells
Scale bars:100 μm
B
Microscope
Flow cytometry
% eGFP-positive cells
αhIgG (-)
(+)
C
% eGFP-positive cells
αhIgG (-)
αhIgG (+)
Vero-E6
Daudi-
D
% eGFP-positive cells
AGS
NU-GC3
Vero-E6
αhIgG (-)
(+)
E
Co-cultured Vero-E6
Akata- EBV-eGFP
eGFP-positive cells
Caveolin-1
Caveolin-1
Scale bars:20 μm
F
Co-cultured Vero-E6
eGFP-positive cells
EBNA1
Scale bars:20 μm

Fig. 2

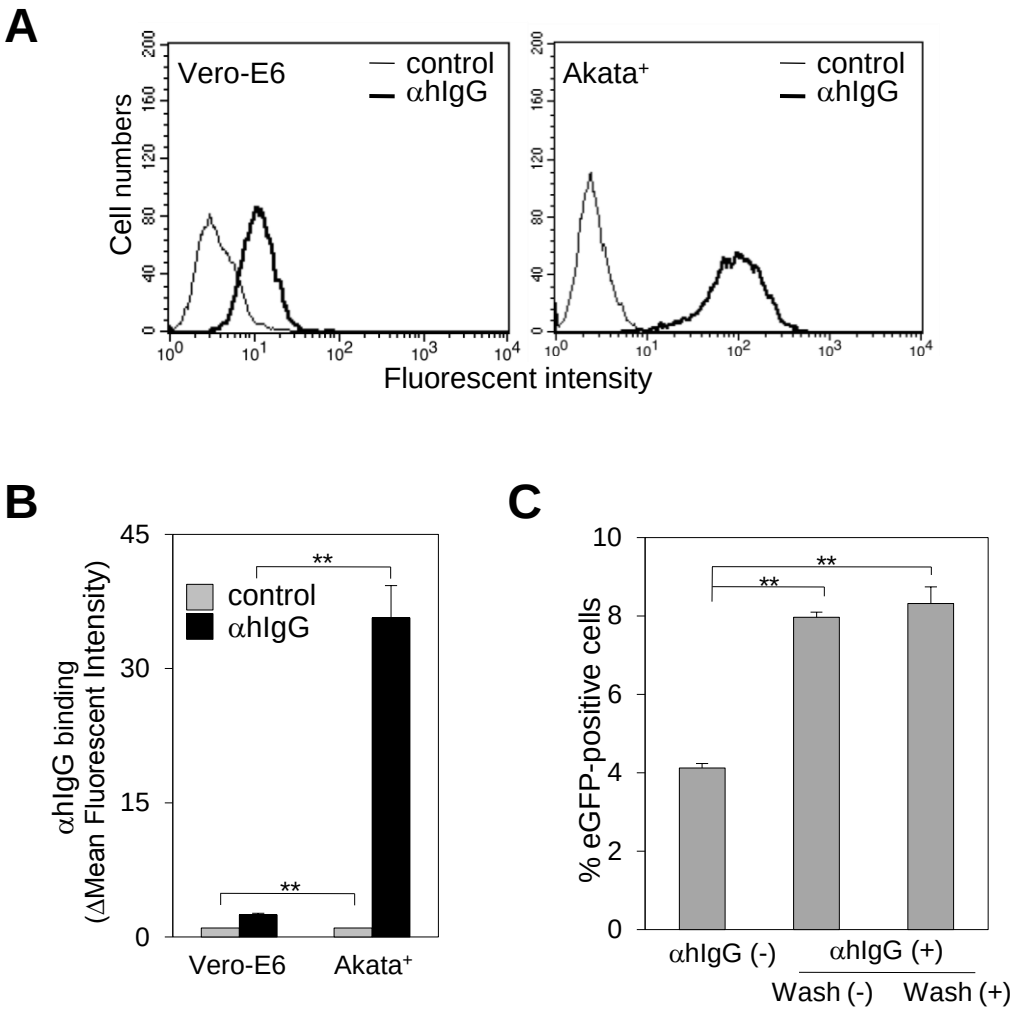
A
Vero-E6
control
αhIgG
Akata+
control
αhIgG
Cell numbers
Fluorescent intensity
B
αhIgG binding
(ΔMean Fluorescent Intensity)
control
αhIgG
**
**
Vero-E6
Akata+
C
% eGFP-positive cells
**
**
αhIgG (-)
αhIgG (+)
Wash (-)
Wash (+)

Fig. 3

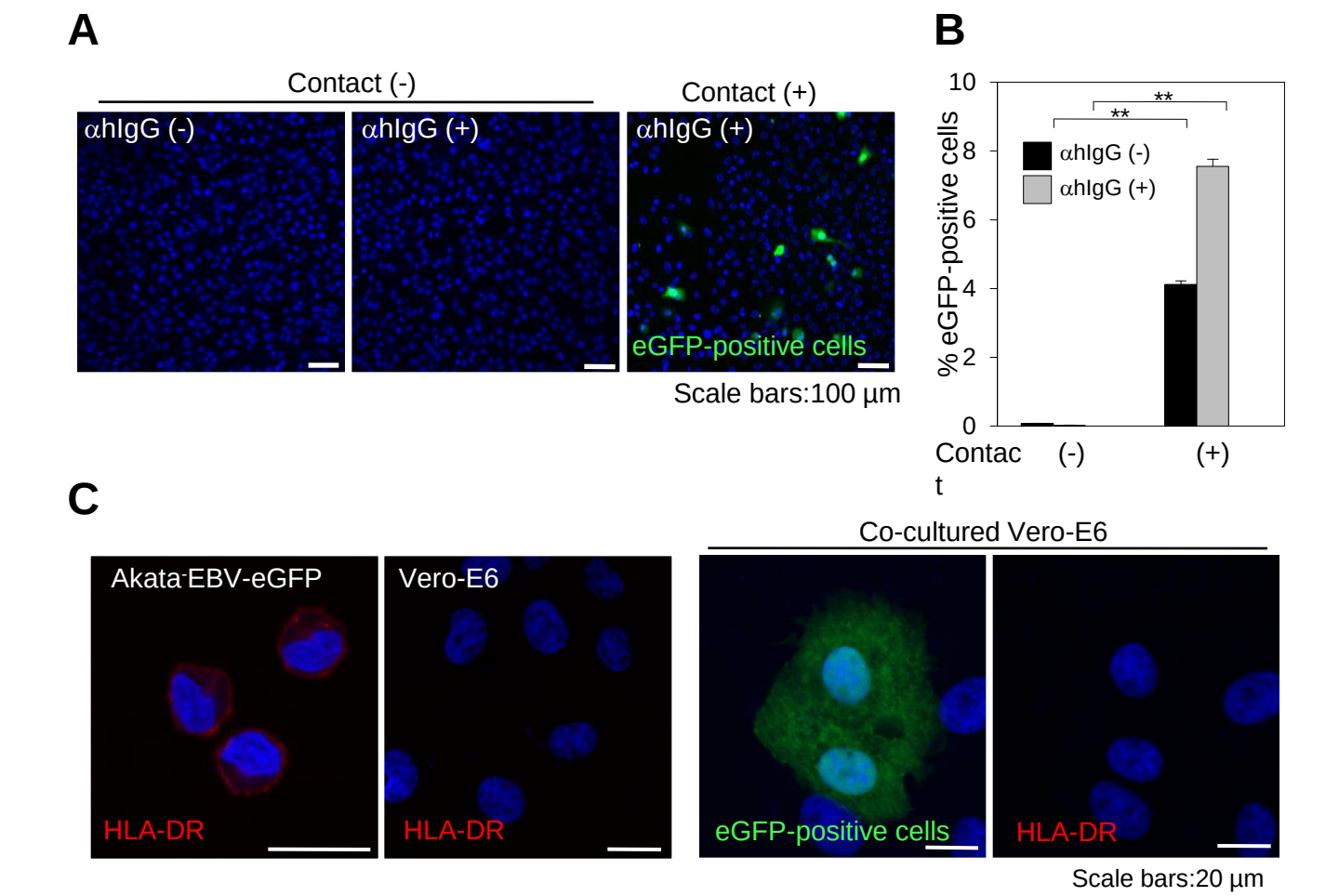
A
Contact (-)
Contact (+)
αhIgG (-)
αhIgG (+)
αhIgG (+)
eGFP-positive cells
Scale bars:100 μm
B
% eGFP-positive cells
αhIgG (-)
αhIgG (+)
**
**
Contact
(-)
(+)
C
Co-cultured Vero-E6
Akata-EBV-eGFP
Vero-E6
HLA-DR
HLA-DR
eGFP-positive cells
HLA-DR
Scale bars:20 μm

Fig. 4

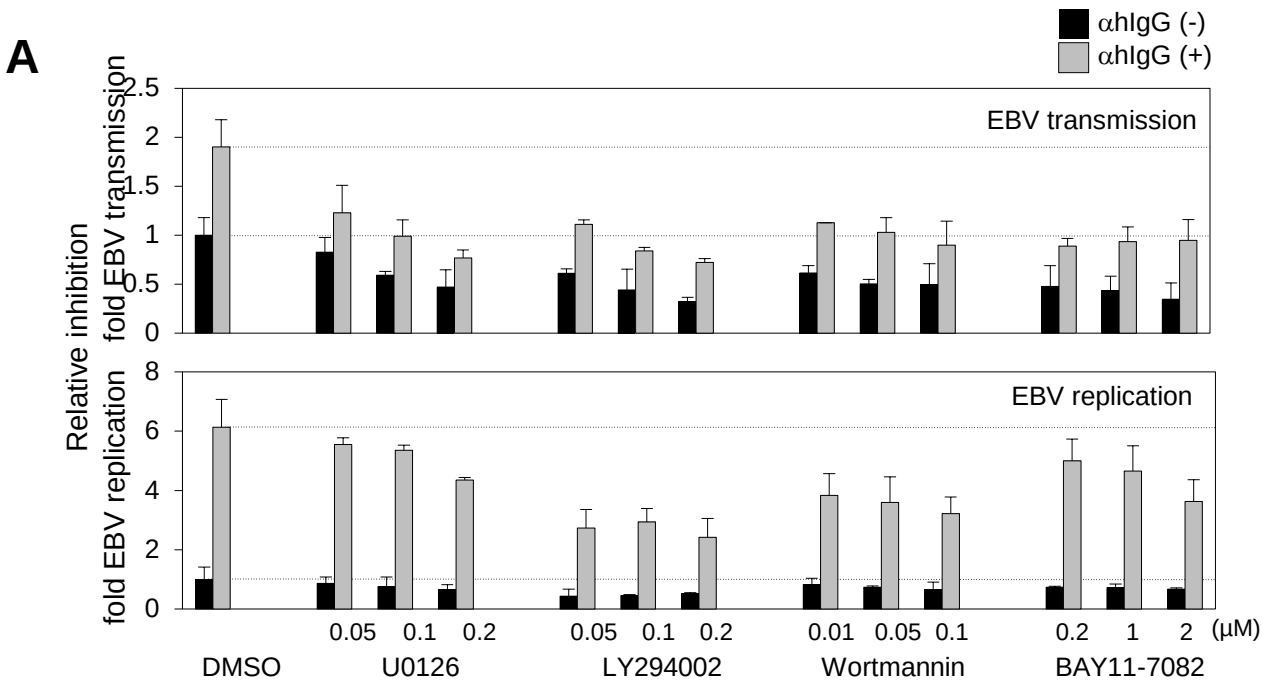
A
αhIgG (-)
αhIgG (+)
EBV transmission
EBV replication
Relative inhibition
fold EBV transmission
fold EBV replication
0.05 0.1 0.2
0.05 0.1 0.2
0.01 0.05 0.1
0.2 1 2 (μM)
DMSO
U0126
LY294002
Wortmannin
BAY11-7082

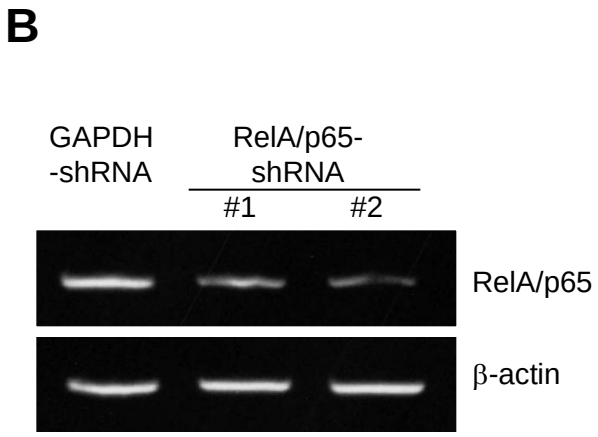
B
GAPDH -shRNA
RelA/p65-shRNA
#1
#2
RelA/p65
β-actin

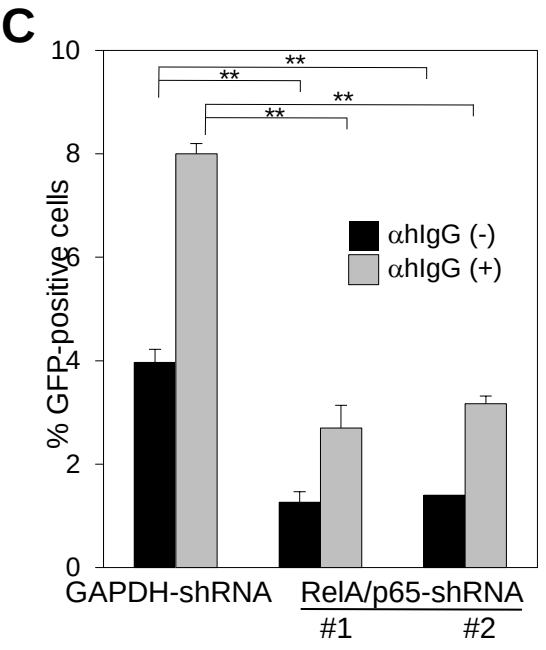
C
% GFP-positive cells
αhIgG (-)
αhIgG (+)
GAPDH-shRNA
RelA/p65-shRNA
#1
#2

Fig. 5

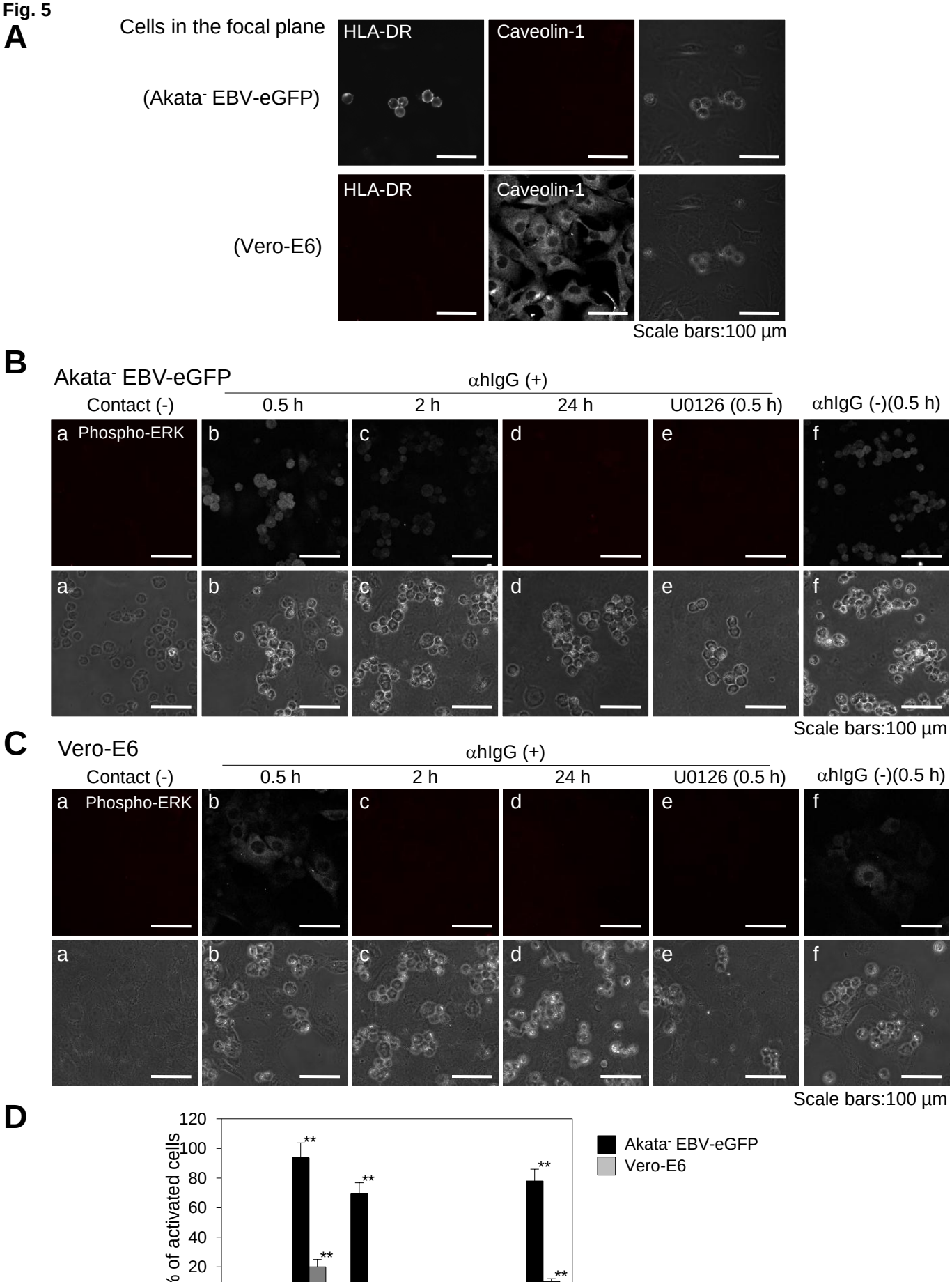
A
Cells in the focal plane
(Akata- EBV-eGFP)
HLA-DR
Caveolin-1
(Vero-E6)
HLA-DR
Caveolin-1
Scale bars:100 μm
B
Akata- EBV-eGFP
αhIgG (+)
Contact (-)
0.5 h
2 h
24 h
U0126 (0.5 h)
αhIgG (-)(0.5 h)
a Phospho-ERK
b
c
d
e
f
Scale bars:100 μm
C
Vero-E6
αhIgG (+)
Contact (-)
0.5 h
2 h
24 h
U0126 (0.5 h)
αhIgG (-)(0.5 h)
a Phospho-ERK
Scale bars:100 μm
D
% of activated cells
120
100
80
60
40
20
0
**
a
b
c
d
e
f
Akata- EBV-eGFP
Vero-E6

Fig. 6

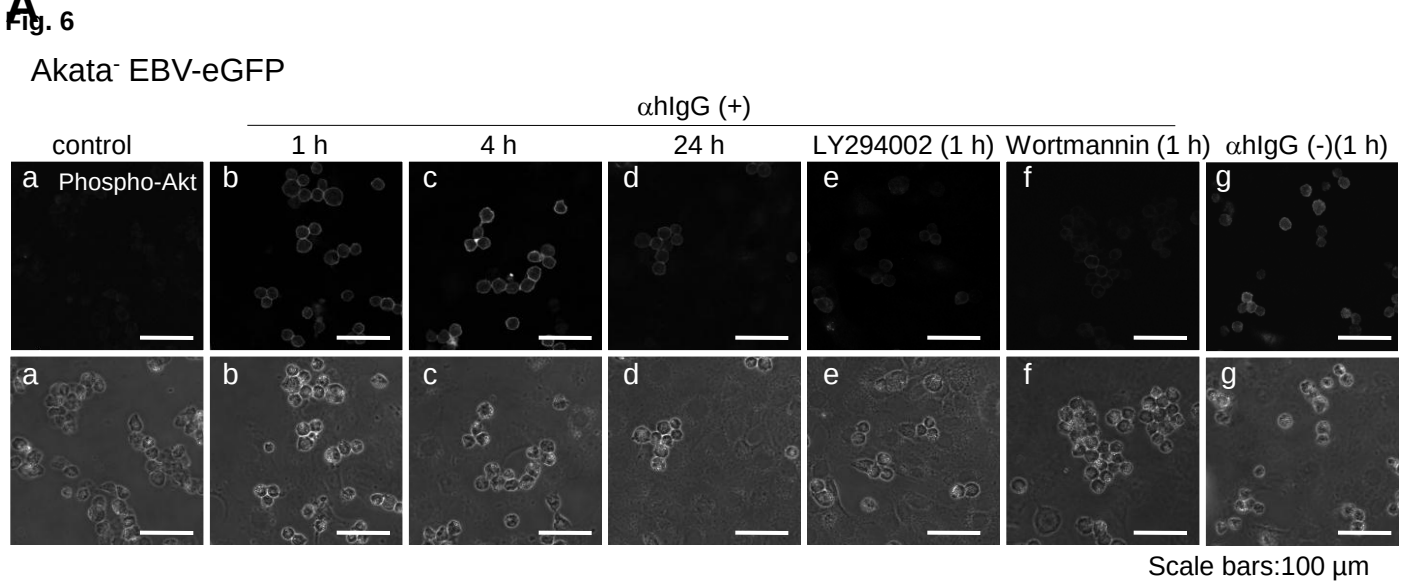
A
Akata- EBV-eGFP
αhIgG (+)
control
1 h
4 h
24 h
LY294002 (1 h)
Wortmannin (1 h)
αhIgG (-)(1 h)
a Phospho-Akt
b
c
d
e
f
g
Scale bars:100 μm

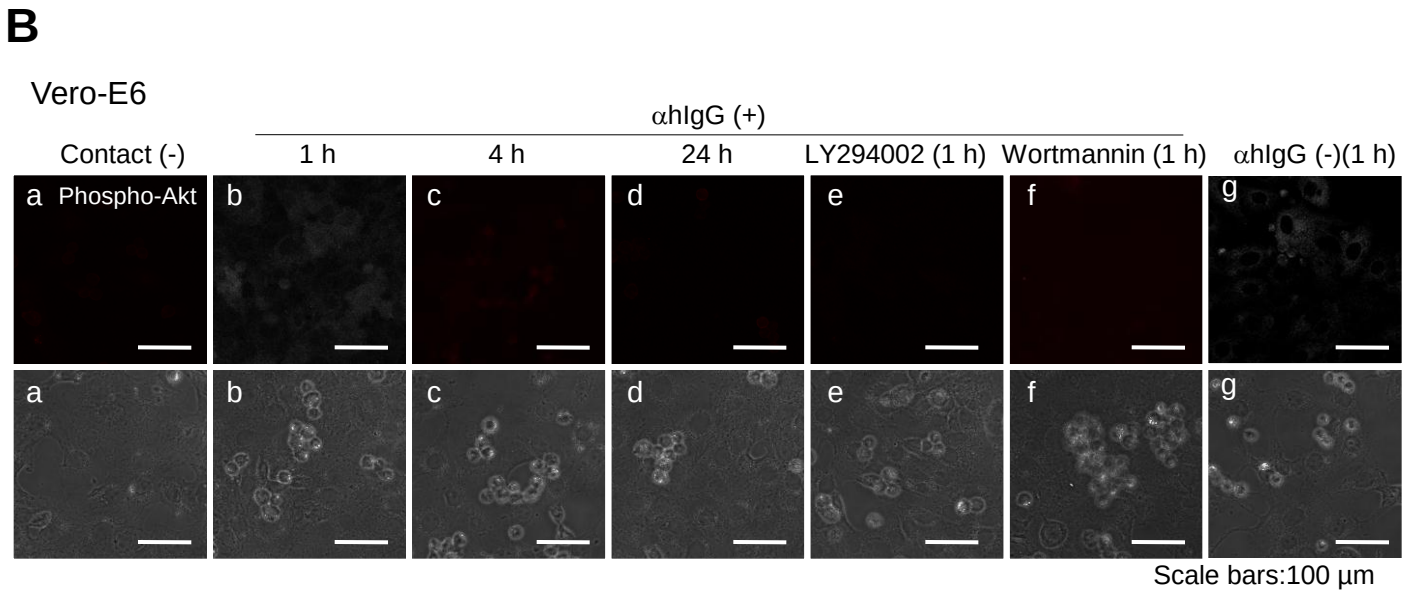
B
Vero-E6
αhIgG (+)
Contact (-)
1 h
4 h
24 h
LY294002 (1 h)
Wortmannin (1 h)
αhIgG (-)(1 h)
a Phospho-Akt
b
c
d
e
f
g
Scale bars:100 μm

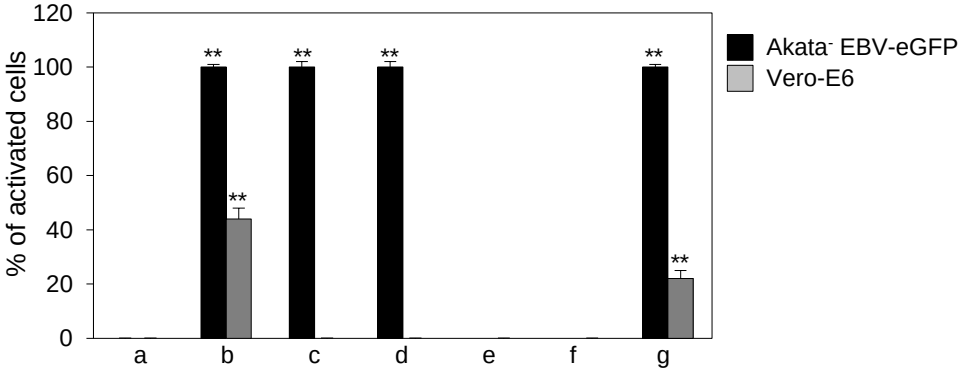
C
% of activated cells
120
100
80
60
40
20
0
**
a
b
c
d
e
f
g
Akata- EBV-eGFP
Vero-E6

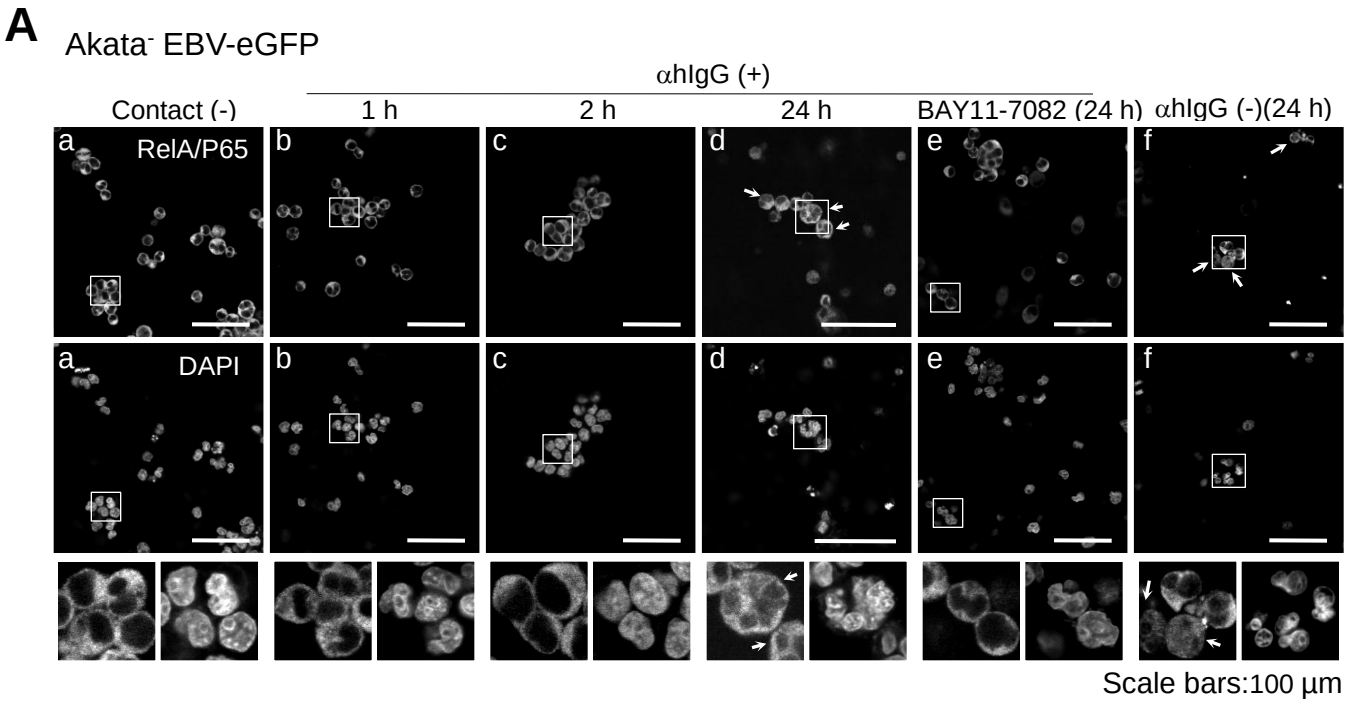
A
Akata- EBV-eGFP
αhIgG (+)
Contact (-)
1 h
2 h
24 h
BAY11-7082 (24 h)
αhIgG (-)(24 h)
RelA/P65
DAPI
Scale bars:100 μm

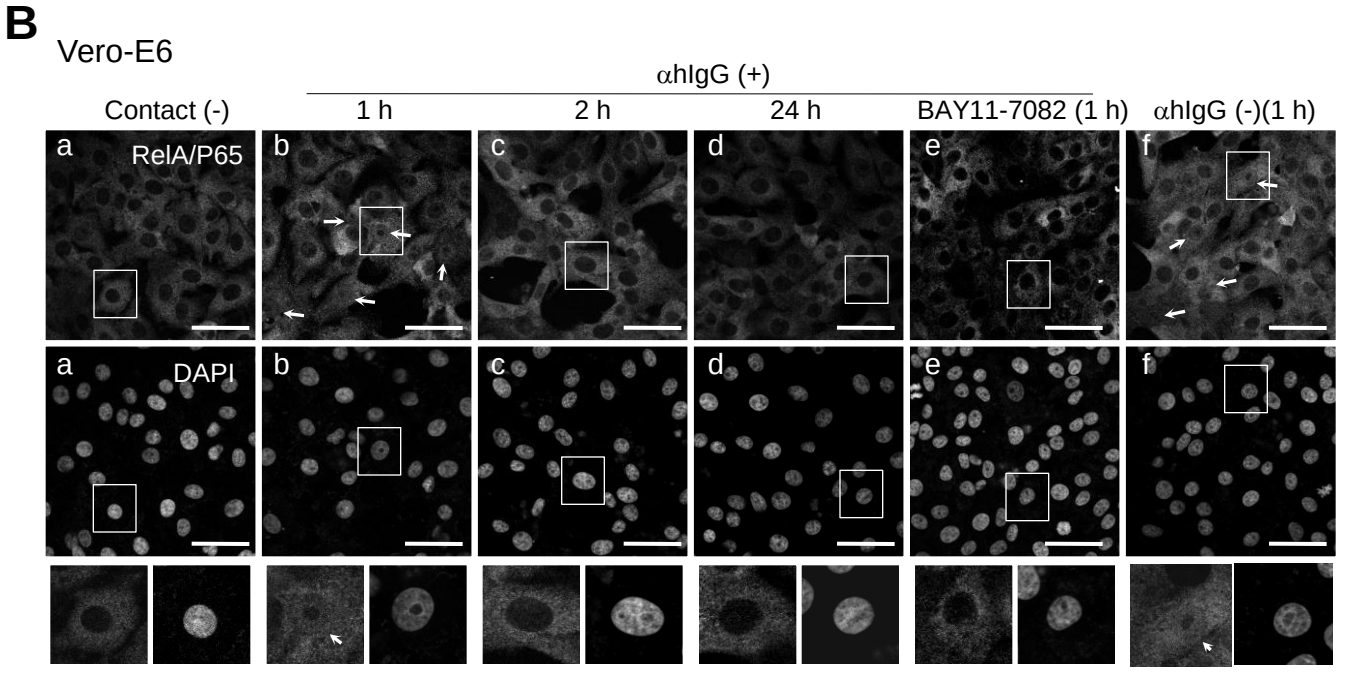
B
Vero-E6
αhIgG (+)
Contact (-)
1 h
2 h
24 h
BAY11-7082 (1 h)
αhIgG (-)(1 h)
RelA/P65
DAPI
Scale bars:100 μm

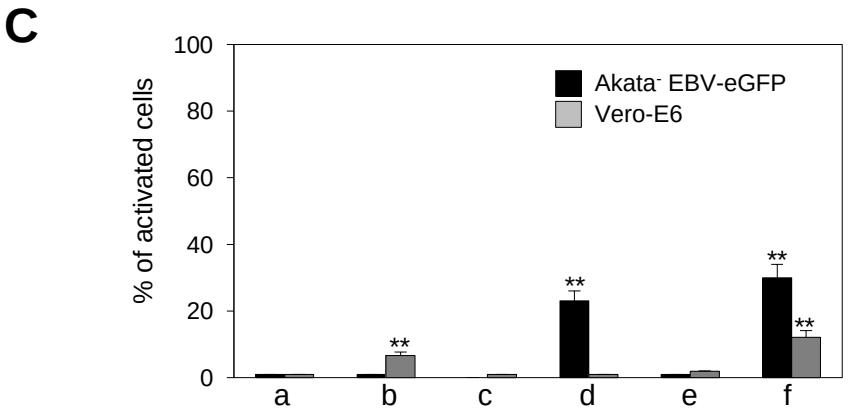
C
% of activated cells
Akata- EBV-eGFP
Vero-E6
100
80
60
40
20
0
a
b
c
d
e
f
**

Fig. 8

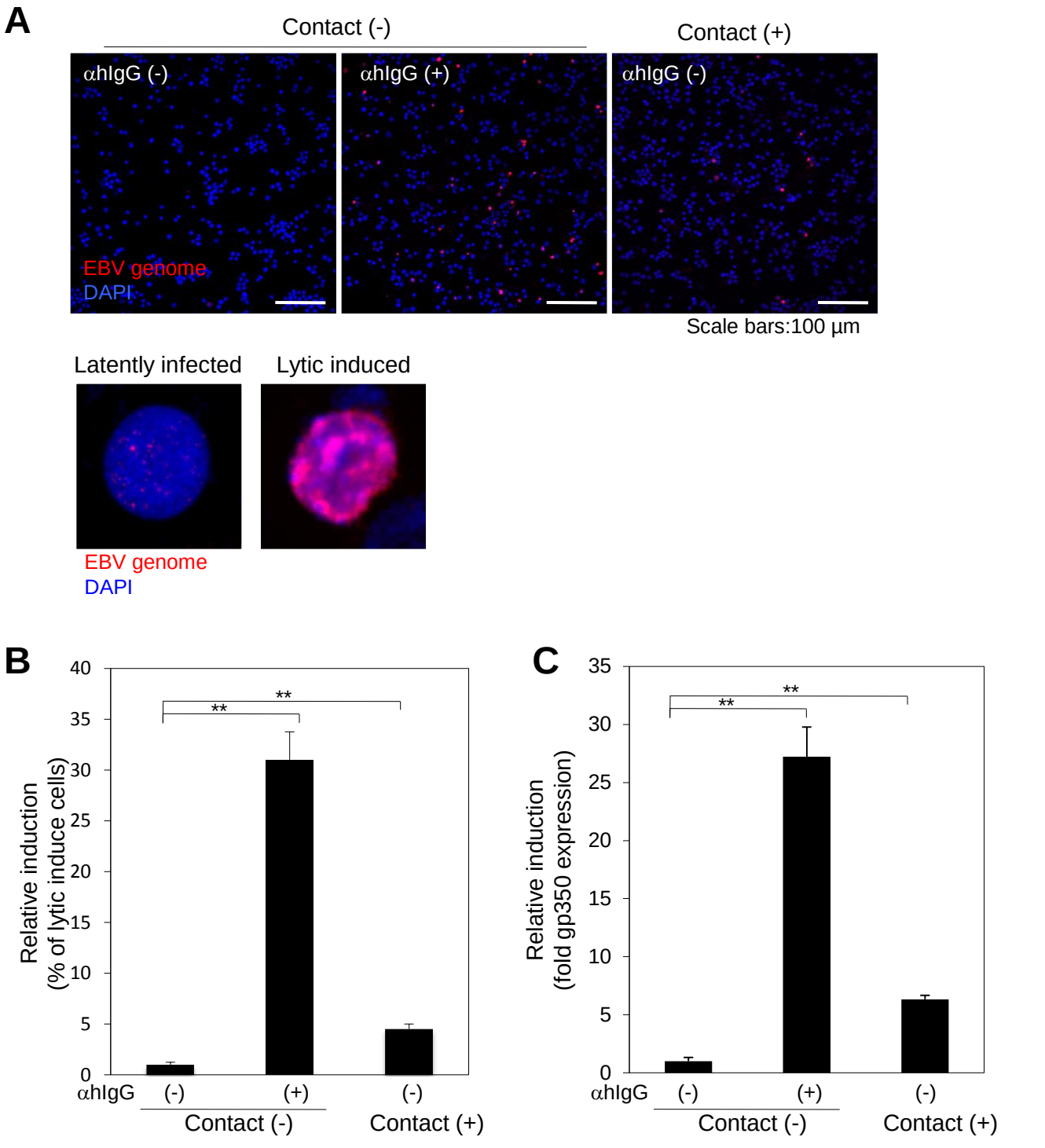
A
Contact (-)
Contact (+)
αhIgG (-)
αhIgG (+)
αhIgG (-)
EBV genome
DAPI
Scale bars:100 μm
Latently infected
Lytic induced
EBV genome
DAPI
B
Relative induction
(% of lytic induce cells)
40
35
30
25
20
15
10
5
0
**
**
αhIgG
(-)
(+)
(-)
Contact (-)
Contact (+)
C
Relative induction
(fold gp350 expression)
35
30
25
20
15
10
5
0
**
**
αhIgG
(-)
(+)
(-)
Contact (-)
Contact (+)